

Density-functional study of interplanar binding in graphite

D. P. DiVincenzo and E. J. Mele

*Department of Physics, University of Pennsylvania, Philadelphia, Pennsylvania 19104
and Laboratory for Research on the Structure of Matter, University of Pennsylvania,
Philadelphia, Pennsylvania 19104*

N. A. W. Holzwarth

Corporate Research-Science Laboratories, Exxon Research and Engineering Company, Linden, New Jersey 07036

(Received 6 October 1982)

Density-functional theory is applied to study the structural and elastic properties of the weak interplanar bonding in graphite. Using the Thomas-Fermi plus gradient approximation to the kinetic energy and taking the charge density to be a superposition of isolated C planes permit rapid computation of the graphite total energy as a function of plane separation. Values for the lattice constant, compressibility, cohesive energy, and phonon frequencies are obtained and are shown to be largely independent of the details of the in-plane C bonding. Agreement with experiment is qualitatively good, but quantitative discrepancies exist. It is argued that these discrepancies are not due to the charge-density approximation or to the Thomas-Fermi approach, but rather to the marginal applicability of the local density approximation to the exchange and correlation. We find that using a van der Waals point of view for the exchange and correlation does not quantitatively improve the theory; so some intermediate approach appears to be necessary.

I. INTRODUCTION

One of the unique properties of graphite is the two entirely different types of interactions which bind the structure. In the graphite basal plane, the C atoms are held in a two-dimensional hexagonal lattice by strong covalent bonds. These bonds, both σ and π , are highly directional and account for a binding energy on the order of 5 eV/C atom. On the other hand, the C planes are held to each other by much weaker energies (of order 5×10^{-2} eV/C atom) which are not at all covalent or directional. These forces are often taken to be of the "van der Waals" type, and several previous calculations have been based on this assumption.^{1,2} However, this previous work was semiempirical, so that while they have proven useful in fitting to certain experimental results, they cannot explore the fundamental origins of the graphite interplane interactions. In the present work we have investigated a nonempirical description of these interactions within the local-density approximation (LDA). Fully *ab initio* band-structure calculations have been performed for graphite^{3,4} which have obtained excellent results for the electronic charge density near the C-C bonds and far away from the planes⁵; however, these studies did not examine the total energy of the graphite system. Thus the present work represents the first attempt at a fully theoretical description of the weak binding in graphite. Other weak-binding systems

have been studied within the LDA: the rare gases physisorbed on graphite (Refs. 6 and 7), He on Ni,⁸ the rare gases on jellium,⁹ and various molecular solids.¹⁰ The agreement between theory and experiment has generally been asserted to be very good; however, for the most part only ion scattering and thermodynamic experiments are available for these systems,⁷ and they provide only somewhat indirect tests for the theory. Many reliable and unambiguous experimental data on the structural properties of graphite are available for direct comparison with theory (e.g., x-ray diffraction,⁵ low-energy electron diffraction,¹¹ neutron scattering,¹² and hydrostatic pressure^{13,14}). We find that the LDA provides a good qualitative description of the weak interplane binding for graphite. However, quantitative discrepancies do exist between theory and experiment. We argue in Sec. IV that this is indicative of an incipient breakdown of the LDA in the low-electron-density regime. This follows the presentation of our total-energy formalism in Sec. II, and the description of the results of our calculation for graphite in Sec. III.

II. CALCULATION

The lamellar structure of graphite allows us to make a very good estimate of its charge density for different values of the *c*-axis lattice constant without performing a band-structure calculation for each

configuration. In particular, the charge density should be quite accurately given by the superposition of the charge densities of isolated graphite layers. This suggests a greatly simplified approach for obtaining the total energy as a function of c -axis lattice separation. The density-functional theory¹⁵ guarantees that a unique and exact relationship exists between the charge density of any solid and its ground-state total energy. While the exact functional $E_T[\rho]$ is not known, adequate approximations to it have been developed and tested for various solid-state systems.¹⁶⁻¹⁸ Our charge-density construction plus the density-functional approach permit the rapid computation of the total energy and the resulting structural and elastic properties of graphite.

In general, the energy functional can be written as

$$E_T[\rho] = T[\rho] + V[\rho], \quad (1)$$

where T is the many-body kinetic energy and V the many-body potential energy. Approximations to E_T are generally made by estimating T and V separately. One commonly used expression for T is

$$T_S = - \sum_i f_i \int_{\Omega} \psi_i^*(\vec{r}) \nabla^2 \psi_i(\vec{r}) d\vec{r}, \quad (2)$$

the kinetic energy of noninteracting electrons. In (2), f_i are the occupation numbers, Ω denotes the crystal volume, and $\psi_i(\vec{r})$ are the one-electron eigenstates. Here and throughout the paper energies are in rydbergs and lengths in Bohr radii. Since in this present work we wish to use a theory based directly on the charge density

$$\rho(\vec{r}) = \sum_i f_i \psi_i^*(\vec{r}) \psi_i(\vec{r})$$

rather than on the eigenfunctions $\psi_i(\vec{r})$, we will not use Eq. (2). An approximation based on (2) which depends only locally on $\rho(\vec{r})$ is the Thomas-Fermi approximation¹⁹:

$$T_{TF} = \frac{\pi^{4/3} 3^{5/3}}{5} \int_{\Omega} [\rho(\vec{r})]^{5/3} d\vec{r}. \quad (3)$$

T_{TF} is equal to T_S for jellium in which $\rho(\vec{r})$ is constant, and T_{TF} has been used with some success even in systems where $\rho(\vec{r})$ is rapidly varying.²⁰ Improvements to Eq. (3) have generally followed two lines: introduction of nonlocality into T_{TF} ,^{21,22} and addition of correction terms to T_{TF} depending on powers of the gradient of the charge density,²³⁻²⁵

$$T \approx T_{TF} + T^{(1)}[|\nabla\rho|^2] + T^{(2)}[|\nabla\rho|^4] + \dots \quad (4)$$

$T^{(2)}$ and higher terms will not concern us here since they have been shown to be small for a wide variety of systems.¹⁶ $T^{(1)}$ has the form

$$T^{(1)} = \gamma \int_{\Omega} \frac{|\nabla\rho(\vec{r})|^2}{\rho(\vec{r})} d\vec{r}. \quad (5)$$

$T^{(1)}$ has been derived using many different approaches: linear-response theory,¹⁵ density-matrix theory,²¹ and a perturbation theory involving iterated commutators.²⁵ All agree on the functional form of Eq. (5), but the value of γ obtained from these theories is different, ranging from $\gamma = \frac{1}{36}$ to $\frac{1}{4}$. The theories give different γ 's because they each include an average of the higher-order correction terms in a different way. The factor $\gamma = \frac{1}{36}$ appears to be best justified on theoretical grounds; moreover, numerical studies^{16,18} indicate that $\gamma = \frac{1}{36}$ gives the best results for a wide range of real systems. Therefore, we have used $\gamma = \frac{1}{36}$ in the present work.

The potential-energy functional $V[\rho]$ in Eq. (1) is generally approximated by first separating it into an (electrostatic) Coulomb energy and exchange and correlation energies²⁶:

$$V[\rho] = V_C[\rho] + V_{xc}[\rho]. \quad (6)$$

$V_C[\rho]$ is the classical electrostatic energy (see below). The exchange and correlation energies $V_{xc}[\rho]$ are usually approximated by a functional which is local in $\rho(\vec{r})$. We have used the functional proposed by Hedin and Lundqvist,²⁷

$$V_{xc}^{\text{loc}}[\rho] = \int_{\Omega} \rho(\vec{r}) \epsilon_{xc}^{\text{HL}}(\rho) d\vec{r}, \quad (7a)$$

$$\begin{aligned} \epsilon_{xc}^{\text{HL}}(\rho(\vec{r})) = & -\frac{9}{4}\alpha \left[\frac{3}{\pi} \right]^{1/3} [\rho(\vec{r})]^{1/3} \\ & - C \left[(1+x^3) \ln \left[1 + \frac{1}{x} \right] + \frac{x}{2} - x^2 - \frac{1}{3} \right], \end{aligned} \quad (7b)$$

where the parameters $\alpha = \frac{2}{3}$, $C = 0.045$,

$$x = \frac{1}{A} \left[\frac{3}{4\pi} \right]^{1/3} [\rho(\vec{r})]^{-1/3},$$

and $A = 21.0$ have been found to reproduce accurately the many-body exchange and correlation energies for the interacting electron gas. As in the case of the kinetic energy, improvements to the functional in Eq. (7) have been suggested, both of a fully nonlocal type^{21,22} and of the gradient type:

$$V_{xc}[\rho] \approx V_{xc}^{\text{loc}}[\rho] + V_{xc}^{(1)}[|\nabla\rho|] + \dots \quad (8)$$

While many authors have studied $V_{xc}^{(1)}$,²⁸ the most comprehensive and recent work has been by Langreth and Mehl,²⁹ who propose that the form

$$V_{xc}^{(1)}[|\nabla\rho|] = C_1 \int_{\Omega} \frac{|\nabla\rho|^2}{\rho^{4/3}} (2e^{-C_2|\nabla\rho|/\rho^{7/6}} - \frac{7}{9}) d\vec{r} \quad (9)$$

with $C_1 = 4.28 \times 10^{-3}$ and $C_2 = 0.262$ gives an im-

proved value for the exchange and correlation energy of atomic systems.

The other term in the potential energy $V_C[\rho]$ is given by the Coulomb energy of the electron charge $\rho(\vec{r})$ in the field of the ion cores:

$$V_C[\rho] = \sum'_{ij\vec{R}} \frac{Z_i Z_j}{|\vec{r}_i - \vec{r}_j - \vec{R}|} + \int_{\Omega_0} \left[\sum_{i\vec{R}} V_{ion}^i(\vec{r} - \vec{r}_i - \vec{R}) \right] \rho(\vec{r}) d\vec{r} + \int_{\Omega_0} \int_{\Omega} \frac{\rho(\vec{r})\rho(\vec{r}')}{|\vec{r} - \vec{r}'|} d\vec{r} d\vec{r}'. \quad (10)$$

Here \vec{R} denotes the real-space lattice vectors, Ω_0 the unit-cell volume, $V_{ion}^i(\vec{r})$ the ionic (pseudo-) potential of the i th ion in the unit cell, Z_i its charge, and \vec{r}_i its position. We will discuss the evaluation of Eq. (10) in some detail later. To summarize all of the above, we will take the approximate expression for the total-energy functional per unit cell in the solid to be

$$E_T[\rho] = \frac{\pi^{4/3} 3^{5/3}}{5} \int_{\Omega_0} \rho^{5/3} d\vec{r} + \frac{1}{36} \int_{\Omega_0} \frac{|\nabla\rho|^2}{\rho} d\vec{r} + \int_{\Omega_0} \left[\sum_{i\vec{R}} V_{ion}^i(\vec{r} - \vec{r}_i - \vec{R}) \right] \rho(\vec{r}) d\vec{r} + \sum'_{ij\vec{R}} \frac{Z_i Z_j}{|\vec{r}_i - \vec{r}_j - \vec{R}|} + \int_{\Omega_0} \int_{\Omega} \frac{\rho(\vec{r})\rho(\vec{r}')}{|\vec{r} - \vec{r}'|} d\vec{r} d\vec{r}' + \int_{\Omega_0} \rho(\vec{r}) \epsilon_{xc}^{HL}(\rho) d\vec{r} + V_{xc}^{(1)}[|\nabla\rho|]. \quad (11)$$

As mentioned earlier, the use of Eq. (11) is possible for graphite because a very simple prescription suffices to estimate the electronic charge density accurately. We propose that $\rho(\vec{r})$ for graphite planes separated by lattice constant c can be adequately approximated by the superposition of the charge densities of isolated graphite layers, and that the C-ion cores move rigidly with the layers. This approximation is correct to leading order in perturbation theory, and has been confirmed directly, although to a limited extent, by band-structure calculations.^{3,4} Note that we shall not be concerned at all with variations of the in-plane structure of graphite, for which any such superposition scheme would certainly be inaccurate; only interplanar structural properties will be studied here.

The charge density of an isolated graphite layer is calculated using a supercell by the mixed-basis band-structure technique³⁰ using nonlocal norm-conserving pseudopotentials.³¹ This method has been demonstrated to give excellent results for the in-plane charge density⁴ in comparison to x-ray experiments.⁵ This calculation also properly gives an exponentially decaying charge density far from the graphite planes which agrees with a linearized augmented-plane-wave (LAPW) calculation to within 10%.³² We point out that by using this approach, the C-C in-plane bond charge is obtained by a fully quantum-mechanical energy functional rather than by the approximate $E_T[\rho]$ in Eq. (11). Only the small changes in the energy resulting from changing the out-of-plane lattice constant c will be described by $E_T[\rho]$. It should be true that use of the pseudopotential technique will actually improve the

applicability of our approximate $E_T[\rho]$. Since the core kinetic energy is accurately contained by the ionic pseudopotential, the Thomas-Fermi kinetic functional, which is designed for a smoothly varying charge density, need only be applied to the carbon valence charge. Of course, by using this procedure, $\rho(\vec{r})$ is not the function which minimizes $E_T[\rho]$; thus $E_T[\rho]$ is not a variational quantity and, for example, the virial theorem is not exactly satisfied. This does not appear to cause any problems in practice.

For actual calculations, it is most convenient to initially represent the isolated plane-charge density in the Fourier-transform domain: $\rho_{\text{plane}}(\vec{G}_\rho, q)$. Here \vec{G}_ρ are the fixed in-plane reciprocal-lattice vectors, while q is a continuous out-of-plane wave vector. In the supercell approach, we actually obtain $\rho_{\text{plane}}(\vec{G}_\rho, G_z)$ on a discrete set of G_z 's. Since the supercell lattice constant has been taken to be 55% larger than the actual graphite plane-plane separation, these G_z 's are closely spaced.³³ When the Fourier transform is defined with the prefactor $1/\Omega_0$,

$$\rho(\vec{r}) \equiv \frac{1}{\Omega_0} \sum_{\vec{G}_\rho, G_z} e^{i\vec{G} \cdot \vec{r}} \rho(\vec{G}_\rho, G_z), \quad (12)$$

direct interpolation to the continuous variable q becomes possible. [Here $\vec{G} = (\vec{G}_\rho, G_z)$ and $G_z = 2\pi n/c$, $n = \text{integer}$.] The charge density of any stack of graphite planes with overall periodicity at lattice constant c and with planes placed in the unit cell at positions $\vec{r}_1, \vec{r}_2, \dots$, is simply

$$\rho_{Gr}(\vec{G}_p, G_z^c) = \sum_{\vec{r}_i} e^{i\vec{G} \cdot \vec{r}_i} \rho_{\text{plane}}(\vec{G}_p, q = G_z^c). \quad (13)$$

Sufficient convergence has been obtained so long as all Fourier components are kept for $G < 10$ a.u.: in the present work this corresponds to about 3000 G 's, not taking symmetry into account. All of the kinetic, exchange, and correlation parts of the functional of Eq. (11) are then evaluated at the same time. First, $\rho_{Gr}(\vec{G})$ of Eq. (13) is Fourier transformed to $\rho_{Gr}(\vec{r})$ according to (12); likewise, $i\vec{G}\rho_{Gr}(\vec{G})$ is transformed to give $\nabla\rho(\vec{r})$. (A fast-Fourier-transform algorithm is used throughout.) Then the indicated integrals are evaluated numerically by the trapezoidal rule on a uniformly spaced grid of about 4×10^5 points throughout the unit cell. Overall, numerical convergence is at least as good as 2 mRy.

The evaluation of the Coulomb part of Eq. (10) requires greater care. Because of the long range of the Coulomb interaction, the terms as written in (10) are separately divergent, although when taken together they are, of course, finite. That is, all the Coulomb terms may be given in a formally convergent way if they are all written together,

$$\begin{aligned} V_C[\rho] &= \int_{\Omega_0} \int_{\Omega} \frac{\rho_{\text{tot}}(\vec{r})\rho_{\text{tot}}(\vec{r}')}{|\vec{r}-\vec{r}'|} d\vec{r} d\vec{r}' \\ &= \frac{1}{2} \int_{\Omega_0} V_{\text{tot}}(\vec{r})\rho_{\text{tot}}(\vec{r}) d\vec{r}. \end{aligned} \quad (14)$$

Here $V_{\text{tot}}(\vec{r})$ is the Hartree potential corresponding to $\rho_{\text{tot}}(\vec{r})$, which in rydberg units is

$$V_{\text{tot}}(\vec{r}) = 2 \int_{\Omega} \frac{\rho_{\text{tot}}(\vec{r}')}{|\vec{r}-\vec{r}'|} d\vec{r}'. \quad (15)$$

We would like to define $\rho_{\text{tot}}(\vec{r})$ as the sum of a valence part and an ionic core part,

$$\rho_{\text{tot}}(\vec{r}) = \rho_{Gr}(\vec{r}) + \sum_{i\vec{R}} \rho_{\text{ion}}^i(\vec{r} - \vec{r}_i - \vec{R}),$$

where the sum is over the atoms in the solid and

$$V_C^{11} = \int_{\Omega_0} \int_{\Omega} \frac{\rho_1(\vec{r})\rho_1(\vec{r}')}{|\vec{r}-\vec{r}'|} d\vec{r} d\vec{r}' = \frac{4\pi}{\Omega_0} \sum_{\vec{G}}' \frac{|\rho_1(\vec{G})|^2}{G^2} = \frac{4\pi}{\Omega_0} \sum_{\vec{G}}' \frac{|\rho_{Gr}(\vec{G})|^2}{G^2}, \quad (19)$$

where the prime on the sum indicates the exclusion of the $G=0$ term. V_C^{12} is similarly calculated:

$$V_C^{12} = \frac{4\pi}{\Omega_0} \sum_{\vec{G}}' \frac{\rho_1^*(\vec{G})\rho_2(\vec{G})}{G^2} = \frac{1}{2\Omega_0} \sum_{\vec{G}}' \rho_1(\vec{G})V_2(\vec{G}) = \frac{1}{2\Omega_0} \sum_{\vec{G}}' \rho_{Gr}(\vec{G}) \left[\sum_{\vec{r}_i} V_{\text{ion}}^i(\vec{G}) e^{i\vec{G} \cdot \vec{r}_i} \right]. \quad (20)$$

The sum over \vec{r}_i indicates a sum over the atoms in the unit cell. Although $V_{\text{ion}}^i(\vec{G})$ is poorly converged in G space, $\rho_{Gr}(\vec{G})$ provides adequate convergence for Eq. (20). V_C^{22} , on the other hand, cannot be evaluated with G -space techniques because of inadequate convergence. To evaluate V_C^{22} we add and subtract point charges from the atom centers for reasons that we will show momentarily:

$\rho_{\text{ion}}(\vec{r})$ is related through Eq. (15) to the ionic pseudopotential $V_{\text{ion}}(\vec{r})$. This procedure is not strictly correct because the ionic pseudopotential used in our band-structure calculation is nonlocal. However, the only part of this potential which is physically important for interplane binding is $V_{\text{ion}}(r)$ for large r . In this regime the nonlocality is virtually zero, so we find that the results of Eqs. (14) and (15) are insensitive to whether $V_{\text{ion}}(r)$ is taken as the s carbon pseudopotential, the p potential, or some reasonable average of the two.

Having thus established the definition of the total charge $\rho_{\text{tot}}(\vec{r})$, we proceed to the actual evaluation of (14). The general strategy²⁶ is to separate $\rho_{\text{tot}}(\vec{r})$ into several parts, each of which is individually neutral and for which the Coulomb energy is easily calculable. We reparate ρ_{tot} into core and valence parts, maintaining neutrality by adding and subtracting a constant:

$$\begin{aligned} \rho_{\text{tot}}(\vec{r}) &= \rho_1(\vec{r}) + \rho_2(\vec{r}) \\ &= (\rho_{Gr}(\vec{r}) - \bar{\rho}_{Gr}) + \left[\sum_{i\vec{R}} \rho_{\text{ion}}^i(\vec{r} - \vec{r}_i - \vec{R}) + \bar{\rho}_{Gr} \right], \end{aligned} \quad (16)$$

where

$$\bar{\rho}_{Gr} \equiv \frac{1}{\Omega_0} \int_{\Omega_0} \rho_{Gr}(\vec{r}) d\vec{r} = \rho_{Gr}(\vec{G}=0) \quad (17)$$

is the average valence charge density. Because of the bilinearity of $V_C[\rho]$ in ρ , it can be written in terms of ρ_1 and ρ_2 as

$$V_C[\rho] = V_C^{11} + V_C^{22} + 2V_C^{12}, \quad (18a)$$

$$V_C^{ij} \equiv \int_{\Omega_0} \int_{\Omega} \frac{\rho_i(\vec{r})\rho_j(\vec{r}')}{|\vec{r}-\vec{r}'|} d\vec{r} d\vec{r}'. \quad (18b)$$

Since ρ_1 is a smoothly varying function of \vec{r} , its plane-wave expansion is rapidly convergent. Therefore V_C^{11} can be immediately evaluated by the G -space formula,

$$\rho_2(\vec{r}) = \rho_3(\vec{r}) + \rho_4(\vec{r}), \quad (21a)$$

$$\rho_3(\vec{r}) = \sum_{i\vec{R}} \rho_{\text{ion}}^i(\vec{r} - \vec{r}_i - \vec{R}) - \sum_{i\vec{R}} Z_i \delta(\vec{r} - \vec{r}_i - \vec{R}), \quad (21b)$$

$$\rho_4(\vec{r}) = \sum_{i\vec{R}} Z_i \delta(\vec{r} - \vec{r}_i - \vec{R}) + \bar{\rho}_{Gr}. \quad (21c)$$

Here $Z_i = \int_{\Omega} \rho_{\text{ion}}^i(\vec{r}) d\vec{r}$. As in Eq. (18), $V_C^{22} = V_C^{33} + V_C^{44} + 2V_C^{34}$. Now ρ_3 consists of point charges embedded in small neutralizing charge clouds which do not extend beyond the ionic radius. Since these units of charge are spherically symmetric and nonoverlapping, V_C^{33} is independent of the lattice constant. Therefore we do not calculate it. V_C^{34} is easily evaluated directly in real space. Since $\bar{\rho}_{Gr} = -(1/\Omega_0) \sum_i Z_i$,

$$\begin{aligned} V_C^{34} &= \frac{1}{2} \int_{\Omega_0} \rho_4(\vec{r}) V_3(\vec{r}) d\vec{r} = -\frac{\left[\sum_i Z_i \right]}{2\Omega_0} \int_{\Omega_0} \sum_{j\vec{R}} \left[V_{\text{ion}}^j(\vec{r} - \vec{r}_j - \vec{R}) - \frac{2Z_j}{|\vec{r} - \vec{r}_j - \vec{R}|} \right] d\vec{r} \\ &= -\frac{\left[\sum_i Z_i \right]}{2\Omega_0} \sum_j \int_{\Omega} \left[V_{\text{ion}}^j(\vec{r} - \vec{r}_j) - \frac{2Z_j}{|\vec{r} - \vec{r}_j|} \right] d\vec{r}. \end{aligned} \quad (22)$$

The integral is density independent and spherically symmetric, so it is evaluated once numerically as a one-dimensional integral. V_C^{34} only depends on the lattice constant through the unit-cell volume Ω_0 . Finally, V_C^{44} is the energy of a lattice of point charges embedded in a constant neutralizing charge density. The standard Ewald sum expression for this energy is³⁴

$$V_C^{44} = \frac{4\pi}{\Omega_0} \sum_{\vec{G}}' \frac{\left| \sum_i Z_i e^{i\vec{G} \cdot \vec{r}_i} \right|^2 e^{-G^2/4\eta}}{G^2} - \frac{2\sqrt{\eta}}{\sqrt{\pi}} \sum_i Z_i^2 + \sum_{ij\vec{R}}' \frac{Z_i Z_j \text{erfc}(\eta^{1/2} |\vec{R} - \vec{r}_i + \vec{r}_j|)}{|\vec{R} - \vec{r}_i + \vec{r}_j|} - \frac{\pi}{\eta\Omega_0} \sum_{ij} Z_i Z_j. \quad (23)$$

Here $\text{erfc}(x) = (2/\sqrt{\pi}) \int_x^\infty e^{-y^2} dy$. The Ewald parameter η is chosen so that both the G sum and the R sum are rapidly convergent.

To summarize, the final expression used in evaluating the total electrostatic energy is

$$\begin{aligned} V_C[\rho] &= \frac{4\pi}{\Omega_0} \sum_{\vec{G}}' \frac{|\rho_{Gr}(\vec{G})|^2}{G^2} + \frac{1}{\Omega_0} \sum_{\vec{G}}' \rho_{Gr}(\vec{G}) \sum_i V_{\text{ion}}^i(\vec{G}) e^{i\vec{G} \cdot \vec{r}_i} - \frac{\left[\sum_i Z_i \right]}{\Omega_0} \sum_j \int_{\Omega} \left[V_{\text{ion}}^j(\vec{r} - \vec{r}_j) - \frac{2Z_j}{|\vec{r} - \vec{r}_j|} \right] d\vec{r} \\ &+ \frac{4\pi}{\Omega_0} \sum_{\vec{G}}' \frac{\left| \sum_i Z_i e^{i\vec{G} \cdot \vec{r}_i} \right|^2 e^{-G^2/4\eta}}{G^2} - \frac{2\sqrt{\eta}}{\sqrt{\pi}} \sum_i Z_i^2 + \sum_{ij\vec{R}}' \frac{Z_i Z_j \text{erfc}(\eta^{1/2} |\vec{R} - \vec{r}_i + \vec{r}_j|)}{|\vec{R} - \vec{r}_i + \vec{r}_j|} - \frac{\pi}{\eta\Omega_0} \sum_{ij} Z_i Z_j. \end{aligned} \quad (24)$$

We have been able to evaluate Eq. (24) with an overall numerical accuracy of about 2 mRy/unit cell.

III. RESULTS

We have performed the calculations indicated above for a graphite lattice with staggered (*A-B*)

stacking with a unit cell of four atoms. The results for the total energy and its components as a function of the out-of-plane lattice constant c are shown in Fig. 1. We show the total Coulomb energy V_C , the

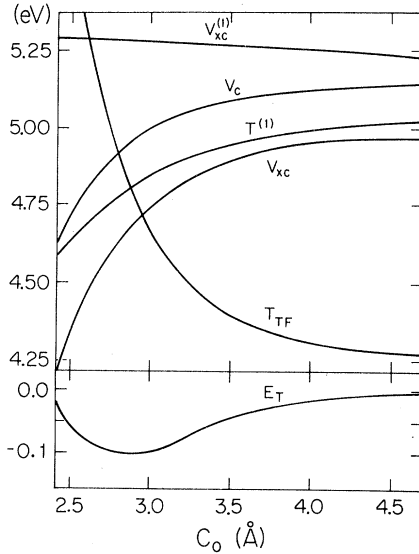


FIG. 1. Calculation of density-functional energies for approximate charge density constructed from superposition of isolated graphite planes. Upper panel: the Thomas-Fermi kinetic energy T_{TF} , the gradient correction to the kinetic energy $T^{(1)}$, the exchange and correlation energies V_{xc} , the gradient correction to the exchange and correlation energies $V_{xc}^{(1)}$, and the electrostatic energy V_C as a function of graphite-layer separation c . Lower panel: total density-functional energy E_T vs c . Energy units are eV/C atom; note the different scales for the upper and lower panels. The energy zeros are arbitrary.

Thomas-Fermi term in the kinetic energy T_{TF} , the gradient correction to the Thomas-Fermi term $T^{(1)}$, the Hedin-Lundqvist local approximation to the exchange and correlation energies V_{xc} , and the gradient correction to the exchange and correlation energies $V_{xc}^{(1)}$. The zero of energy for all of these quantities has been arbitrarily shifted. As the figure shows, the kinetic energy provides a large repulsive barrier to the collapse of the system; this is a universal feature of solid-state systems. Note that because the charge-density gradients are reduced as the lattice constant decreases, the gradient correction to the kinetic energy makes this barrier somewhat smaller. As expected, the exchange and correlation forces between graphite planes are attractive, leading to the upward slope of $V_{xc}(c)$. The gradient correction to this energy, $V_{xc}^{(1)}$, is found to be negligible. Perhaps the most surprising feature of Fig. 1 is the magnitude of the attractive electrostatic energy V_C . Despite the fact that this energy represents the Coulomb energy between individually neutral planes at a fairly long distance, its magnitude is not insignificant compared with the other energies in the problem. This is at variance with the typical point of view of the graphite-graphite plane interactions,²

and we will devote more discussion to it later.

Figure 1 also gives the resulting total energy E_T as a function of the c -axis lattice constant. As the figure shows, the variations of E_T are small compared with the variations of its components. Our results give a positive binding energy for AB graphite, with a stable minimum at $c_0 = 2.80$ Å, about 15% smaller than the experimental value $c_0 = 3.35$ Å. At this minimum point, the compressibility is given by

$$k_c = \frac{A_0}{c_0} \left[\frac{\partial^2 E_T}{\partial c^2} \right]^{-1},$$

where A_0 is the unit-cell area in the graphite basal plane. Our theory gives $k_c = 0.97 \times 10^{-12}$ cm²/dyn, about a factor of 3 smaller than experiment.³⁵ (For a detailed comparison of theory and experiment see Table I.) While the agreement with experiment in this work is certainly not as good as in energy density-functional theories for metals,³⁶ or for simple semiconductors,³⁷ it is the sort of agreement which has been found in Kohn-Sham³⁸ studies of the intermolecular properties of other molecular solids.³⁹ Thus, while the present results are not in perfect quantitative agreement with experiment, they are qualitatively correct: They place the C-C plane separation at a distance much larger than distances typical for strong covalent bonding (for C-C, 1.42 Å), with a larger compressibility than is typical for strongly bonded materials. We will say more about this point later.

Further comparison between theory and experiment are shown in the table. To facilitate this comparison, we have fitted both our theoretical results and the experimental results for the equation of state,^{13,14} elastic constants,^{12,34} and heat of wetting¹ by a Morse curve,⁴⁰

$$E_T(c) = b_1 (e^{-b_2(c-b_3)} - 1)^2. \quad (25)$$

The values of b_i are given in the table. The fit to the theoretical points is essentially perfect, and the fit to the composite of experiments is quite good; hence it seems that Eq. (25) is an appropriate fitting form. The difference in the theoretical and experimental b_i 's reflects the above-mentioned discrepancy in the equilibrium elastic properties. The total C-C plane cohesive energy is given by the parameter b_1 . The theoretical value, $E_T(c \rightarrow \infty) - E_T(c = c_0)$, is found to be 8 mRy/C atom. The experimental value, extracted in an indirect way from calorimetric surface wetting measurements,¹ is about 5 times smaller. Note that our theory does predict that the carbon interplane bonding is much weaker than the intraplane binding energies, which are of the order of 10^3 mRy/C atom. The other parameter of the Morse function, b_2 , gives the decay length of the to-

TABLE I. Morse-potential parameters and structural and elastic constants for graphite for the density-functional theory using three different charge-density approximations and for experiment.

	Superposition of graphite planes	Theory Superposition of C atoms	Homogeneous exponential sheet model	Experiment
Morse parameters				
b_1 (meV/unit cell)	439	762	427	91 ^a
b_2 (\AA^{-1})	0.837	0.558	0.656	0.971 ^b
b_3 (\AA)	5.58	5.99	5.65	6.69 ^b
Structural parameters				
Plane binding energy				
E_B (meV/C atom)	110	191	107	23 ^a
Compressibility				
k_c (cm^2/dyn)	0.97×10^{-12}	1.18×10^{-12}	1.6×10^{-12}	2.7×10^{-12c}
Optic shear frequency				
$\omega_{E_{2g}}$ (cm^{-1})	40.8	20.6	0	42 ± 1^d

^aReference 1.

^bReferences 13 and 14.

^cReference 12.

^dReference 40.

tal energy towards zero. Theory and experiment agree fairly well on this parameter; this implies that, for example, the trend of experimental equation-of-state data^{13,14} is well reproduced theoretically.

We have also investigated the stability of other plane-stacking sequences for lattice constant $c = c_0$. We find *AB* stacking to be more stable than *AA* stacking by 3.4 mRy/C atom. In fact, we find *AB* stacking to be the most stable among all the two-layer repeat stackings in agreement with experiment. Also, by studying the appropriate rigid-phonon displacement, we are able to predict the frequency of the low-lying E_{2g} optic shear mode in graphite. This is a mode in which alternate graphite planes move in opposite directions in the x - y plane. Our calculation gives $\omega_{E_{2g}} = 40.8 \text{ cm}^{-1}$. While this is in perfect agreement with experiment,⁴¹ such agreement is admittedly fortuitous in view of the other inaccuracies of the calculation. Still, our theory reveals an interesting feature of this shear mode; it is found to be strongly anharmonic. This anharmonicity should be manifested as an observable increase of this frequency under hydrostatic pressure. This possibility has not been studied experimentally.

In order to discover how sensitive the above results are to small modifications in our theory, we have evaluated the energy-functional equation (11) for a different $\rho(\vec{r})$, one formed simply by the superposition of neutral pseudoatom densities:

$$\rho_{Gr}(\vec{r}) = \sum_{i, \vec{R}} \rho_{\text{atom}}(\vec{r} - \vec{r}_i - \vec{R}). \quad (26)$$

Here $\rho_{\text{atom}}(\vec{r})$ is the outer-shell charge density of the neutral isolated C atom obtained from the norm-conserving pseudopotential technique.³¹ The density in Eq. (26) is very similar to that obtained from the superlattice band-structure density far away from the atomic planes, but they are naturally very different near the C bonds.⁴ Thus this calculation will show us how sensitive the interlayer binding is to changes in the near-plane charge density.

Figure 2 shows the results of the density-functional calculation on $\rho_{Gr}(\vec{r})$ in Eq. (26). The behavior of the various components of the total energy in Fig. 2 is both qualitatively and quantitatively similar to the corresponding ones in Fig. 1. The resulting total-energy curve is also quite similar to that obtained with the band-structure density. While the numerical predictions for the binding energy, compressibility, and shear frequency are different in this approximation (see the table for this comparison), the qualitative feature of weak binding is unchanged, and the predicted lattice constant is only changed by 5%. We conclude that even rather substantial errors in the in-plane features of the charge density leave the important interplane results of the energy-functional calculation largely unaffected.

This conclusion has encouraged us to study an even more drastic approximation to the graphite charge density, one in which the in-plane structure is removed altogether. That is, we replace the carbon ions by δ -function sheets,

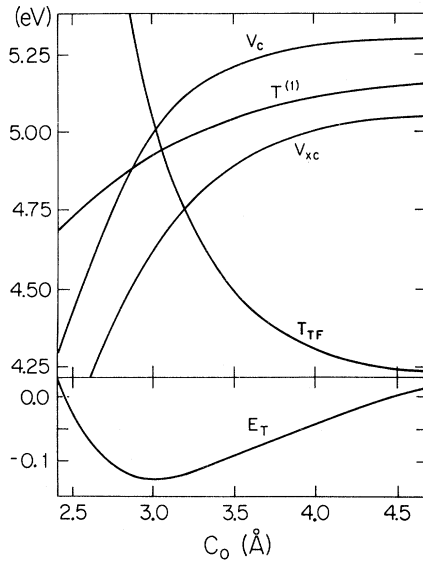


FIG. 2. Same as Fig. 1, calculated for approximate $\rho(\vec{r})$ constructed from superposition of neutral C atoms. $V_{xc}^{(1)}$ is not obtained.

$$\rho_{\text{ion}}(\vec{r}) = - \sum_{i\vec{R}} \frac{cZ_i}{\Omega_0} \delta(z - z_0), \quad (27)$$

and the graphite valence charge by a sum of exponential charge densities with no in-plane variation,

$$\rho_{Gr}(\vec{r}) = \sum_{i\vec{R}} \frac{Z_i}{2a} e^{-|(z - \vec{R} \cdot \hat{z} - \vec{r}_i \cdot \hat{z})/a|}. \quad (28)$$

Figure 3 shows that Eq. (28) provides a good match far from the graphite planes to both the superlattice band structure $\rho_{Gr}(\vec{r})$ [Eqs. (12) and (13)] and the superposition of atoms $\rho_{Gr}(\vec{r})$ [Eq. (26)] if the exponential decay constant $a = 1.23$ Å. The simplicity of this model permits analytic solutions to be obtained for several of the components of the energy functional, which consequently aids in understanding the nature and origin of these components. For example, the electrostatic energy is given in this model by

$$V_C = \frac{2\pi a \left[\sum_i Z_i \right]^2 c}{\Omega_0} \left[\coth(\beta) - \frac{\beta}{\sinh^2(\beta)} \right], \quad (29)$$

where $\beta = c/2a$. This function actually agrees with the V_C calculated with the more accurate $\rho_{Gr}(\vec{r})$ quite well. That is, the change in Coulomb energy upon changing the lattice constant c has almost nothing to do with the in-plane structure of the charge. This shows that the Coulomb energy should be thought of as arising from the direct overlap of

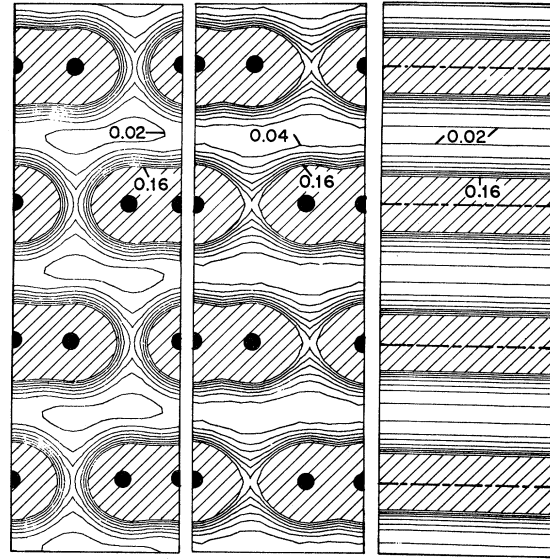


FIG. 3. Three different charge-density approximations shown in a cut perpendicular to the graphite planes passing through the C—C bonds. Graphite stacking is AB. Contour values are in $e/\text{Å}^3$; regions where the charge density is greater than $0.16 e/\text{Å}^3$ are shaded. Left panel: superposition of isolated plane charge densities. Middle panel: superposition of neutral C atoms. Right panel: homogeneous exponential sheet model [Eqs. (27) and (28)]. In this model the C ions are modeled by δ -function sheets shown as dotted-dashed lines.

charges on different planes, rather than from the long-range quadrupole-quadrupole interaction between C—C bonds on neighboring planes. In fact, we have found by direct calculation that this quadrupole-quadrupole contribution is small. We have also evaluated analytically the gradient contribution to the kinetic energy within this isotropic plane model; it is given by

$$T^{(1)} = \frac{2 \sum_i Z_i}{36a} \left[1 - \frac{\tan^{-1}[\sinh(\beta)]}{\sinh(\beta)} \right]. \quad (30)$$

Again, we find this to be in good quantitative agreement with the calculation of Fig. 1, showing that the in-plane charge corrugations are irrelevant to the interplanar gradient energy. Figure 4 shows V_C and $T^{(1)}$ as a function of lattice constant c , along with the other energy-functional components and total energy as in Eq. (11), all according to the charge density of Eqs. (27) and (28). The numerical agreement of these with all the corresponding curves in Figs. 1 and 2 is striking. A parallel set of values for the various equilibrium properties appears in the table; these numbers are again in good agreement with those from the more complex calculations (ex-

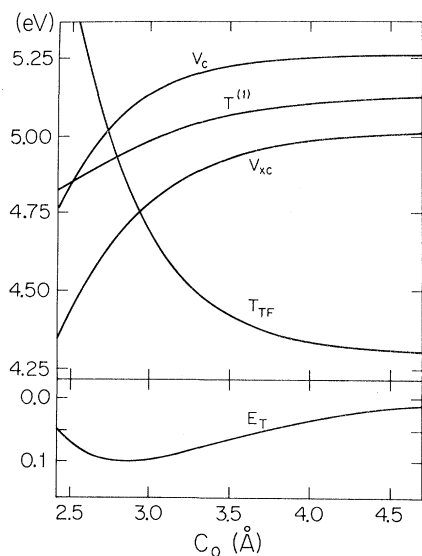


FIG. 4. Same as Fig. 1 calculated for homogeneous exponential sheet model. $V_{xc}^{(1)}$ is not obtained.

cept, of course, the layer shear frequency, which is nonzero only because of the in-plane graphite structure).

IV. DISCUSSION

As the preceding section has shown, the results of the density-functional calculation provide a reasonable qualitative description of the interplane binding of graphite. The quantitative accuracy of this description, however, is poorer than in many other solid-state systems to which density-functional theory has been applied.^{9,10,15,17,18,36,37,39} We now attempt to uncover the source of this quantitative discrepancy, and we predict that no currently studied theory within the density-functional framework is capable of providing completely accurate predictions for the interplane properties of graphite.

The most obvious source of error in the present calculation is inaccuracy in the creation of the graphite charge density. We have already discarded this problem to a certain extent by showing that the superposition of atoms results are only slightly different from those of the superposition of planes. What remains is to show that small variations in the exponentially decaying charge density far from the graphite planes will not cause larger changes in the results of the theory. As mentioned earlier, the exponential decay constant in the pseudopotential band-structure calculation used here differs by about 10% from that found in a surface LAPW calculation for graphite.³² Therefore we have studied the effect of varying the exponential decay length of the

out-of-plane charge using our simplest charge-density model containing only δ -function sheets with exponential electronic charge densities [Eqs. (27) and (28) and Fig. 3]. Figure 5 shows the variation of the equilibrium z -axis lattice parameter c and the total energy E_T with the decay constant a . c has an extremum for a near 1.23 Å, the theoretical decay constant; therefore, the binding properties vary very little with a , and small errors in it should have little effect on the density-functional predictions. In addition to this, Fig. 5 brings out a number of other interesting properties. First, it shows that the equilibrium lattice constant c is reduced substantially both for larger and smaller a . That is, a layered material with either a more or less diffuse charge density than graphite will have closer plane binding, whereas carbon provides a charge-density decay which results in the largest possible lattice constant. Another feature of Fig. 5 is that the approximate density-functional total energy is variationally minimized near $a = 1.23$ Å. Thus both the approximate semiclassical E_T and the quantum-mechanical E_T possess minima near the same value of a , suggesting that we have made an accurate approximation of the Kohn-Sham³⁸ functional.

In fact, we have a more direct way of demonstrating that the use of the Thomas-Fermi plus gradient approximation for the kinetic energy gives results essentially identical to the one-particle kinetic-energy approximation as used in the supercell band structure. We are able to directly evaluate both T_S and $T_{TF} + T^{(1)}$ [Eqs. (2) and (4)] for the graphite planes at the supercell separation. We find T_S and $T_{TF} + T^{(1)}$ to agree if the prefactor of the $T^{(1)}$ term, γ [see Eq. (5)], is taken to be $6 (\frac{1}{36})$. This is larger

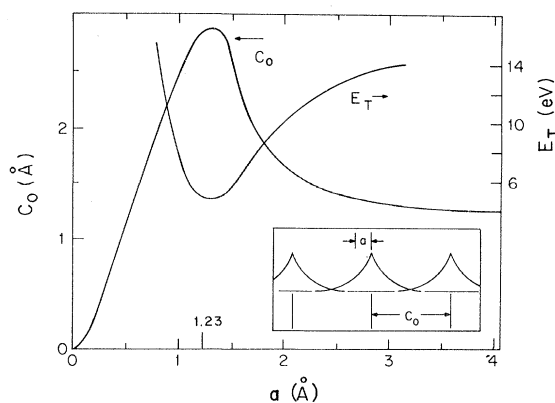


FIG. 5. Equilibrium lattice constant c_0 and the total energy at equilibrium E_T as a function of variations of the decay constant a in the homogeneous electron sheet model. The inset depicts the charge density along the z axis in this model.

than $\gamma = \frac{1}{36}$ which we use in our density-functional calculations because it takes into account the correction to the Thomas-Fermi kinetic energy both near the C planes and in the interstitial volume. Near the C planes the charge density is rapidly varying, so the $T^{(1)}$ prefactor is predicted to be near $9 \left(\frac{1}{36}\right)$.^{21,23} Far from the atomic planes the charge density is smoothly varying, so $\gamma = \frac{1}{36}$.^{15,24,25} Thus $\gamma = 6\left(\frac{1}{36}\right)$ is quite a reasonable spatial average of these two limiting cases. Still, $\gamma = \frac{1}{36}$ is most appropriate in our calculations since the region near mid-gap is most important for interplane binding, as the distribution of $\Delta T^{(1)}(\vec{r})$ along the z axis (Fig. 6) shows. [$\Delta T^{(1)}(\vec{r})$ corresponds to the integrand of Eq. (5), with the contribution from infinitely separated planes subtracted out.] So, on the whole, the factor $\gamma = \frac{1}{36}$ seems well justified, and there is every reason to believe that this kinetic-energy approximation should not cause substantial errors in the predictions of the ground-state properties of graphite. We particularly point out that the elimination of $T^{(1)}$ (i.e., $\gamma=0$) has been a common procedure in other work.^{6,10,19} Although this procedure has given good results for other molecular solids,¹⁰ the present calculation indicates that this procedure would be theoretically unjustified. For graphite, using $\gamma=0$ results in binding which is much weaker than experiment. (A similar problem was encountered by Freeman⁶ in a study of Ar on graphite.)

In fact, a separate total-energy calculation on another molecular solid, Se, performed previously with a state-of-the-art density-functional band-

structure theory, gives results for intermolecular binding which disagree with experiment to a similar extent as this work³⁹; for example, the intermolecular Se lattice constant is underestimated by 10% in the theory. Therefore we conclude that the local-density approximation itself shows evidence of breaking down quantitatively (but not qualitatively) for graphite and similar materials with very weak charge overlaps. This conclusion does not conflict with earlier results that the LDA gives an accurate description of physisorption of, for example, Xe on jellium.⁹ In that case, the physisorption distance was 5 a.u. (cf. 7 au. for the graphite lattice constant), and the charge overlap was about 10% compared with 1% for graphite. Thus for overlaps somewhere between these two cases, the LDA apparently ceases to be quantitatively accurate.

It would seem that the local point of view to electronic correlation across the graphite planes is not strictly correct and must be somewhat modified. We thus have compared the local exchange and correlation energies with the van der Waals² energy. This energy is calculated with the opposite assumption about correlation by considering perturbations about complete localization of the electronic eigenstates from plane to plane. We have calculated the leading term for the van der Waals interaction between two graphite planes separated by distance c to be⁴²

$$V_{\text{vdw}} = \frac{-3A_0}{128\pi^2 c^4} \int_0^\infty [\chi(q \rightarrow 0, iu)]^2 du, \quad (31)$$

where $\chi(q, \omega)$ is the two-dimensional polarizability of a graphite plane.⁴³ Because of V_{vdw} 's strong depen-

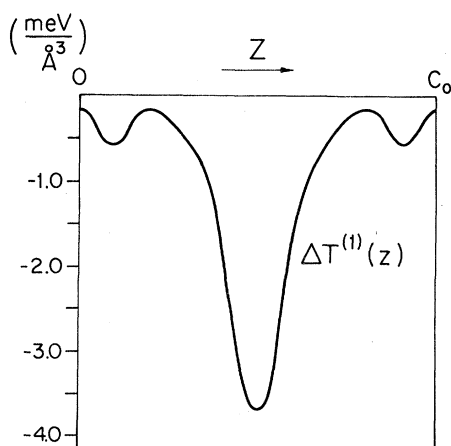


FIG. 6. $\Delta T^{(1)}(z)$, the gradient correction to the kinetic energy, averaged in the x - y plane with the contribution from infinitely separated planes subtracted. Calculated for the superposition of the plane charges model with $c = 2.79 \text{ \AA}$. Note that the magnitude of $\Delta T^{(1)}(z)$ is largest midway between the C planes.

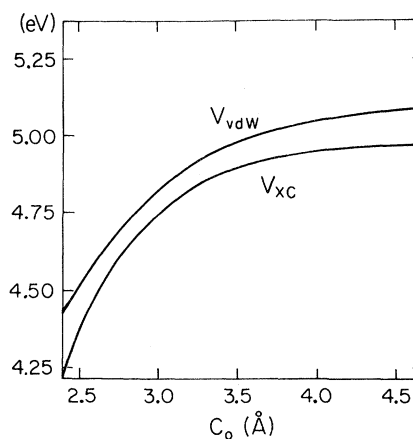


FIG. 7. Comparison of the LDA approximation to the exchange and correlation energies V_{xc} with the van der Waals approximation V_{vdw} as a function of plane separation c . Note the strong similarity between the two curves.

dence on c , contributions to this energy from second-, third-, etc., neighbor planes are negligible. Figure 7 compares V_{vdw} and V_{xc} [Eq. (7)] as a function of c . They are remarkably similar, and including either V_{vdw} or V_{xc} in the complete density-functional theory leads to predictions in quantitative disagreement with experiment. So neither of these two extreme points of view provides an entirely satisfactory account of interlayer cohesion. Some intermediate point of view between localization and complete delocalization seems to be required. No such density-functional theory embodying this intermediate point of view is currently in use, so graphite

should provide a fruitful area of testing for future advances in this area of theory.

ACKNOWLEDGMENTS

We thank Professor S. Rabii and Professor J. E. Fischer for many helpful conversations. We acknowledge the use of the IBM 4341 computer at the Department of Physics at the University of Pennsylvania. This work was supported by the National Science Foundation, Materials Research Laboratory program under Grant No. DMR-79-23647.

- ¹L. A. Girifalco and R. A. Lad, *J. Chem. Phys.* **25**, 693 (1956).
- ²R. O. Brennan, *J. Chem. Phys.* **20**, 40 (1952).
- ³R. C. Tatar and S. Rabii, *Phys. Rev. B* **25**, 4126 (1982).
- ⁴N. A. W. Holzwarth, S. G. Louie, and S. Rabii, *Phys. Rev. B* **26**, 5382 (1982), and in *Proceedings of the Symposium on Local Density Approximations in Quantum Chemistry and Physics, Copenhagen, Denmark, 1982*, edited by J. P. Dahl and J. Avery (Plenum, New York, 1983).
- ⁵R. Chen, P. Trucano, and R. F. Stewart, *Acta Crystallogr. Sect. A* **33**, 823 (1977).
- ⁶D. L. Freeman, *J. Chem. Phys.* **62**, 941 (1975).
- ⁷M. W. Cole, D. R. Frankl, and D. L. Goodstein, *Rev. Mod. Phys.* **53**, 199 (1981).
- ⁸D. R. Hamann, *Phys. Rev. Lett.* **46**, 1227 (1981).
- ⁹N. D. Lang and A. R. Williams, *Phys. Rev. B* **25**, 2940 (1982), and references therein.
- ¹⁰R. LeSar and R. G. Gordon, *Phys. Rev. B* **25**, 7221 (1982).
- ¹¹N. J. Wu and A. Ignatiev, *Phys. Rev. B* **25**, 2983 (1982).
- ¹²R. Nicklow, W. Wakabayashi, and H. G. Smith, *Phys. Rev. B* **5**, 4951 (1972).
- ¹³H. G. Drickamer, *Science* **156**, 1183 (1967).
- ¹⁴P. W. Bridgeman, *Proc. Am. Soc. Arts Sci.* **76**, 9 (1945).
- ¹⁵P. Hohenberg and W. Kohn, *Phys. Rev.* **136**, B864 (1964).
- ¹⁶C. Q. Ma and V. Sahni, *Phys. Rev. B* **16**, 4249 (1977).
- ¹⁷J. K. Norskov and N. D. Lang, *Phys. Rev. B* **21**, 2131 (1980), and references therein.
- ¹⁸J. R. Chelikowsky, *Phys. Rev. B* **21**, 3074 (1980).
- ¹⁹E. H. Lieb, *Rev. Mod. Phys.* **53**, 603 (1981).
- ²⁰C. Muhlhausen and R. G. Gordon, *Phys. Rev. B* **24**, 2147 (1981); **24**, 2161 (1981), and references therein.
- ²¹J. A. Alonso and L. A. Girifalco, *Phys. Rev. B* **17**, 3735 (1978); J. A. Alonso and L. C. Balbas, *Phys. Lett.* **81A**, 467 (1981).
- ²²O. Gunnarson, M. Jonson, and B. Lundqvist, *Phys. Rev. B* **20**, 3136 (1980).
- ²³G. F. von Weizsacher, *Z. Phys.* **96**, 431 (1935).
- ²⁴L. L. DeRaad, Jr. and J. Schwinger, *Phys. Rev. A* **25**, 2399 (1982), and references therein; W. Wang, R. G. Parr, R. Murphy, and G. Henderson, *Chem. Phys. Lett.* **43**, 409 (1976).
- ²⁵D. A. Kirzhnits, *Zh. Eksp. Teor. Fiz.* **32**, 115 (1957) [*Sov. Phys.—JETP* **5**, 64 (1957)]; C. H. Hodges, *Can. J. Phys.* **51**, 1428 (1973); D. R. Murphy, *Phys. Rev. A* **24**, 1682 (1981).
- ²⁶The following discussion parallels somewhat that of M. T. Yin and M. L. Cohen, *Phys. Rev. B* **26**, 3259 (1982); J. Ihm, Alex Zunger, and Marvin L. Cohen, *J. Phys. C* **12**, 4409 (1979); **13**, 3095(E) (1980).
- ²⁷L. Hedin and B. I. Lundqvist, *J. Phys. C* **4**, 2664 (1971).
- ²⁸J. Herman, J. P. van Dyke, and I. B. Ortenburger, *Phys. Rev. Lett.* **22**, 807 (1969); D. C. Langreth and J. P. Perdew, *Phys. Rev. B* **21**, 5469 (1980), and references therein.
- ²⁹D. C. Langreth and M. L. Mehl, *Phys. Rev. Lett.* **47**, 446 (1981).
- ³⁰S. G. Louie, K. M. Ho, and M. L. Cohen, *Phys. Rev. B* **19**, 1774 (1979).
- ³¹D. R. Hamann, M. Schluter, and C. Chiang, *Phys. Rev. Lett.* **43**, 1494 (1979).
- ³²R. B. Laughlin (unpublished).
- ³³The supercell lattice constant was chosen in connection with a study of the electronic structure of Ba-intercalated graphite. The C—C bond length in this structure is different than in pure graphite by an insignificant amount ($\sim 1\%$).
- ³⁴W. A. Harrison, *Pseudopotentials in the Theory of Metals* (Benjamin, New York, 1966), p. 166; K. Fuchs, *Proc. R. Soc. London Ser. A* **151**, 585 (1935).
- ³⁵H. Zabel and A. Magerl, *Phys. Rev. B* **25**, 2463 (1982), and references therein.
- ³⁶P. K. Lam and M. L. Cohen, *Phys. Rev. B* **24**, 4224 (1981); A. R. Williams, J. Kubler, and C. D. Gelatt, *ibid.* **19**, 6094 (1979).
- ³⁷M. T. Yin and M. L. Cohen, *Phys. Rev. B* **25**, 4317 (1982), and references therein.
- ³⁸W. Kohn and L. J. Sham, *Phys. Rev.* **140**, A1133 (1965).

³⁹J. Joannopoulos (private communication).

⁴⁰S. Rabi, Phys. Rev. B 17, 4104 (1978).

⁴¹R. J. Nemanich, G. Lucovsky, and S. A. Solin, in *Proceedings of the International Conference on Lattice Dynamics, Paris, 1977*, edited by M. Balkanski (Flam-

marion, Paris, 1978), p. 619.

⁴²E. Zaremba and W. Kohn, Phys. Rev. B 13, 2270 (1976).

⁴³E. J. Mele and J. J. Ritsko, Phys. Rev. B 24, 1000 (1981).